

# Quark-gluon vertex dressing and meson masses beyond ladder-rainbow truncation.

Hrayr H. Matevosyan,<sup>1,2,3</sup> Anthony W. Thomas,<sup>2</sup> and Peter C. Tandy<sup>4</sup>

<sup>1</sup>*Louisiana State University, Department of Physics & Astronomy,  
202 Nicholson Hall, Tower Dr., LA 70803, USA*

<sup>2</sup>*Thomas Jefferson National Accelerator Facility,  
12000 Jefferson Ave., Newport News, VA 23606, USA*

<sup>3</sup>*Laboratory of Theoretical Physics, JINR, Dubna, Russian Federation*

<sup>4</sup>*Center for Nuclear Research, Department of Physics, Kent State University, Kent, Ohio 44242, USA*

(Dated: July 4, 2019)

We include a generalized infinite class of quark-gluon vertex dressing diagrams in a study of how dynamics beyond the ladder-rainbow truncation influences the Bethe-Salpeter description of light quark pseudoscalar and vector mesons. The diagrammatic specification of the vertex is mapped into a corresponding specification of the Bethe-Salpeter kernel, which preserves chiral symmetry. This study adopts the algebraic format afforded by the simple interaction kernel used in previous work on this topic. The new feature of the present work is that in every diagram summed for the vertex and the corresponding Bethe-Salpeter kernel, each quark-gluon vertex is required to be the self-consistent vertex solution. We also adopt from previous work the effective accounting for the role of the explicitly non-Abelian three gluon coupling in a global manner through one parameter determined from recent lattice-QCD data for the vertex. With the more consistent vertex used here, the error in ladder-rainbow truncation for vector mesons is never more than 10% as the current quark mass is varied from the u/d region to the b region.

PACS numbers: 12.38.Aw; 11.30.Rd; 12.38.Lg; 12.40.Yx

## I. INTRODUCTION

In recent years there has been significant progress in the study of the spectrum of hadrons, and their non-perturbative structure and form factors, through approaches that are manifestly covariant and which accommodate both dynamical chiral symmetry breaking (DCSB) and quark confinement [1]. Covariance provides efficient and unambiguous access to form factors [2, 3, 4]. Consistency with chiral symmetry and its spontaneous breaking is obviously crucial to prevent the pseudoscalars from artificially influencing the difficult task of describing and modeling the infrared dynamics; this is a role better left to other hadronic states that are not so dominated by chiral symmetry. The associated concept of a constituent quark mass is important and it is often implemented in models as a constant mass appearing in the propagator; however this idealization runs into trouble for higher lying states where the sum of the constituent masses is below the hadron mass. This difficulty is marginally evident with the  $\rho$ , but it is inescapable by the time one has

reached the ground state axial vector mesons (e.g.,  $a_1$ ,  $b_1$  mesons) [5].

In reality, solutions of the QCD equation of motion for the quark propagator (quark Dyson-Schwinger equation (DSE)) give a momentum-dependent quark mass function that evolves from the current mass value at ultraviolet spacelike momenta to a value some 0.4 GeV larger in the deep infrared [6]. This is driven by the same mechanism as DCSB and has an important influence over the low-lying hadron spectrum. In the chiral limit, the scalar term of the quark self-energy, which shows most of this evolution, plays a dual role as the dominant invariant amplitude of the chiral pion Bethe-Salpeter equation (BSE) amplitude at low momenta [7]. In any process where the spatial extent of the pion plays an important role (e.g., the charge form factor) the running of the quark mass function is likewise crucial to an efficient symmetry-preserving description. Otherwise a theoretical model is fighting symmetries. It is this large value of the dressed quark mass function at low spacelike momentum that leads, in model solutions of the quark DSE, to  $|p^2| \neq M^2(p^2)$  within a significant domain of timelike momenta where these models can be trusted. For example, this is sufficient to prevent spurious  $q\bar{q}$  production thresholds in light quark hadrons below about 2 GeV [5].

The task of maintaining manifest covariance, DCSB, a running quark mass function and an explicit substructure in terms of confined quarks is often met by models defined as truncations of the DSEs of QCD [1, 8, 9]. For practical reasons the equations must be truncated to decouple arbitrarily high order n-point functions from the

---

Notice: This manuscript has been authored by The Southeastern Universities Research Association, Inc. under Contract No. DE-AC05-84150 with the U.S. Department of Energy. The United States Government retains and the publisher, by accepting the article for publication, acknowledges that the United States Government retains a non-exclusive, paid-up, irrevocable, world wide license to publish or reproduce the published form of this manuscript, or allow others to do so, for United States Government purposes.

set of low order n-point functions used to construct observables. A common truncation scheme is the rainbow-ladder truncation. Here the one-loop gluon dressing of the quark (with bare gluon-quark vertices) is used self-consistently to generate the quark propagator. In general the kernel  $K$  of the Bethe-Salpeter equation is given in terms of the quark self-energy  $\Sigma$  by a functional relation dictated by chiral symmetry [10]. This preserves the Ward-Takahashi identity for the color singlet axial vector vertex and ensures that chiral pseudoscalars will remain massless, independent of model details. With a rainbow self-energy, this relation yields the ladder BSE kernel. To go beyond this level, one needs to realize that the exact quark self-energy is given by the same structure except that one of the gluon-quark vertices is fully dressed. It is the vertex dressing that generates the terms in  $K$  beyond ladder level. This is the topic we are concerned with in this paper.

The ladder BSE for meson bound states is an integral equation with a one-loop kernel structure that must allow for the spinor structure of propagators and the meson amplitudes. With the four-dimensional space-time that one must use to maintain manifest covariance, and with dynamically generated quark propagators that one must use to preserve the Ward-Takahashi identities of chiral symmetry, the numerical task is large. Any scheme for corrections to the ladder truncation will in general add the complexity of multiple loop Feynman diagrams involving amplitudes that are only known after solution. For practical reasons the studies that have been able to investigate hadron states beyond ladder-rainbow truncation in recent years [11, 12, 13, 14] have exploited the simplifications following from use of the Munczek-Nemirovsky (MN) model [15]. In this case the basic element is a delta function in the exchanged (or gluon) momentum; it reduces both the quark DSE and the meson BSE to algebraic equations. There is only one parameter—a strength set by  $m_\rho$ . This simplification preserves the dominant features of quark DSE solutions of realistic models: large infrared strength giving DCSB and the (confining) absence of a mass pole. Of course, the MN model misrepresents the ultraviolet and one must be wary of its use for related physics. Bound state masses are relatively safe in this regard.

The first study of the correction to ladder-rainbow truncation was made in this context in Ref. [11] where a one-gluon exchange dressing of the quark-gluon vertex was implemented for pseudoscalar and vector mesons and scalar and axial vector diquark correlations. Subsequently [12] it was realized that the algebraic structure allowed a recursive implementation of the ladder series of diagrams for the quark-gluon vertex as well as an implementation of the corresponding series of diagrams for the chiral symmetry-preserving BSE kernel. So far as we are aware this was the first solution of a BSE equation in which the kernel contained the effects from an infinite number of loops. In these works the chiral pseudoscalars remained massless independent of the model parameter,

$m_\rho$  received corrections of order 10% from ladder dressing of the vertex, and the diquark states evident at ladder-rainbow level were removed from the spectrum by the dressing effects. The influence of vertex dressing upon the quark propagator was also studied.

There is very little in the way of guidance from realistic non-perturbative non-Abelian models of the infrared structure of the quark-gluon vertex. It has often been assumed, e.g., see Ref. [16], that a reasonable beginning is the Ball-Chiu [17] or Curtis-Pennington [18] Abelian Ansatz times the appropriate color matrix. These Abelian descriptions of the momentum dependence satisfy the Abelian vector Ward-Takahashi identity, and their use makes the implicit assumption that this might be a good enough approximation to the corresponding identity for QCD, namely the Slavnov-Taylor identity for the color octet vertex [19]. The use of an explicit ladder sum for the gluon vertex provides easy access to the chiral symmetry preserving BSE kernel and receives some motivation from the fact that a ladder-summed photon-fermion vertex combines with the rainbow approximation for the fermion propagator to preserve the Ward-Takahashi identity for that vertex.

However when initial results from lattice-QCD simulations of the gluon-quark vertex became available [20, 21], it was realized [22] that the color algebra generated by any ladder sum for this vertex gives a magnitude and strength for the dominant amplitude at zero gluon momentum that is qualitatively and quantitatively incompatible with the lattice data and incompatible with the leading ultra-violet behavior of the one-loop QCD Slavnov-Taylor identity. The infrared vertex model developed in Ref. [22] made an extension of the fact that the one-loop QCD color structure introduced by the three-gluon coupling repairs the deficiency of a purely ladder structure. The color structure of the ladder class of diagrams produces a weak repulsive vertex, while the color structure of the three-gluon coupling contribution produces an attractive contribution that is enhanced by a factor of  $-N_c^2$  at the purely one-loop level.

These observations from Ref. [22] were blended with the algebraic features afforded by the MN model to re-examine the relation between vertex dressing, the chiral symmetry-preserving BSE kernel, and the resulting meson spectrum and diquark correlations [14]. This approach introduced one extra parameter (besides the gluon 2-point function strength and the quark current mass)—an effective net color factor fitted to lattice-QCD data on the gluon-quark vertex. The net attraction in the vertex, driven by the explicitly non-Abelian 3-gluon coupling, had a marked effect: the ladder-rainbow truncation made  $m_\rho$  30% too high compared to the solution from the completely summed vertex. In other words, the attraction produced by summed vertex dressing in a non-Abelian context is more important than previously thought. However in that approach, the structure of the vertex is such that the coupling of any internal gluon line to a quark, is itself bare. This is not self-consistent

and one can question what effect this omitted infinite sub-class of vertex dressing and BSE kernel contributions may have upon the hadron spectrum.

In the present work we extend the analysis of Ref. [14] by the incorporation of a wider class of vertex dressing diagrams. We allow the coupling of any internal gluon line to a quark to be described by the dressed vertex at an order consistent with a given total order in the final vertex. In the limit of the vertex summed to all orders, this becomes the use of the self-consistent quark-gluon vertex at every internal location in a diagram. We borrow from previous work the use of the MN model of the 2-point gluon function to generate an algebraic structure and we again incorporate the important non-Abelian three-gluon coupling through the device of an effective net color factor refitted to the lattice data for the vertex. We use the infinite series of diagrams for the BSE kernel generated from the chiral symmetry-preserving relation to the quark self-energy. We investigate the resulting spectrum of pseudoscalar and vector mesons.

In Section II we describe general properties of the quark-gluon vertex and the relationship with the associated BSE kernel that preserves chiral symmetry. Information from the Slavnov-Taylor identity for the gluon-quark vertex and the Ward-Takahashi identity for the color singlet axial-vector vertex is summarized for relevance to present considerations. We discuss diagrammatic summations that have been used previously to model the gluon vertex and the generalized class of diagram considered here. In Section III we introduce the interaction model that allows an algebraic analysis and we present consequent results for the gluon-quark vertex and the self-consistent dressed quark propagator. The associated symmetry-preserving BSE kernel is presented also. Section IV contains a presentation and analysis of the methods and results for the meson masses. In Section V there is a summary.

## II. THE QUARK-GLUON VERTEX AND THE BETHE-SALPETER KERNEL

We employ Landau gauge and a Euclidean metric, with:  $\{\gamma_\mu, \gamma_\nu\} = 2\delta_{\mu\nu}$ ;  $\gamma_\mu^\dagger = \gamma_\mu$ ; and  $a \cdot b = \sum_{i=1}^4 a_i b_i$ . The dressed quark-gluon vertex for gluon momentum  $k$  and quark momentum  $p$  can be written  $ig t^c \Gamma_\sigma(p+k, p)$ , where  $t^c = \lambda^c/2$  and  $\lambda^c$  is an SU(3) color matrix. In general,  $\Gamma_\sigma(p+k, p)$  has 12 independent invariant amplitudes. We are particularly concerned in this work with the vertex at  $k = 0$ , in which case the general form is

$$\begin{aligned} \Gamma_\sigma(p) = & \alpha_1(p^2) \gamma_\sigma + \alpha_2(p^2) \gamma \cdot p p_\sigma - \alpha_3(p^2) i p_\sigma \\ & + \alpha_4(p^2) i \gamma_\sigma \gamma \cdot p \end{aligned} \quad (1)$$

where  $\alpha_i(p^2)$  are invariant amplitudes. In the model studies of Refs. [12] and [14] that we build upon, one finds  $\alpha_4 = 0$ ; this will also be the case here.

As we shall discuss later, we wish to utilize the functional relation that enables the BSE kernel to be generated from the quark self-energy so that chiral symmetry is preserved. This requires the vertex to be represented in terms of a set of explicit Feynman diagrams. Some exact results are known for the vertex at 1-loop order in QCD [23]. In Landau gauge and to  $\mathcal{O}(g^2)$ , i.e., to 1-loop, the amplitude  $\Gamma_\sigma$  is given by

$$\Gamma_\sigma^{(1)}(p+k, p) = Z_1 \gamma_\sigma + \Gamma_\sigma^A(p+k, p) + \Gamma_\sigma^{\text{NA}}(p+k, p), \quad (2)$$

with

$$\begin{aligned} \Gamma_\sigma^A(p+k, p) = & -(C_F - \frac{C_A}{2}) \int_q^\Lambda g^2 D_{\mu\nu}(p-q) \gamma_\mu \\ & \times S_0(q+k) \gamma_\sigma S_0(q) \gamma_\nu, \end{aligned} \quad (3)$$

and

$$\begin{aligned} \Gamma_\sigma^{\text{NA}}(p+k, p) = & -\frac{C_A}{2} \int_q^\Lambda g^2 \gamma_\mu S_0(p-q) \gamma_\nu D_{\mu\mu'}(q+k) \\ & \times i \Gamma_{\mu'\nu'\sigma}^{3g}(q+k, q) D_{\nu'\nu}(q), \end{aligned} \quad (4)$$

where  $\int_q^\Lambda = \int^\Lambda d^4 q / (2\pi)^4$  denotes a loop integral regularized in a translationally-invariant manner at mass-scale  $\Lambda$ . Here  $Z_1(\mu^2, \Lambda^2)$  is the vertex renormalization constant to ensure  $\Gamma_\sigma = \gamma_\sigma$  at renormalization scale  $\mu$ . The following quantities are bare: the three-gluon vertex  $ig f^{abc} \Gamma_{\mu\nu\sigma}^{3g}(q+k, q)$ , the quark propagator  $S_0(p)$ , and the gluon propagator  $D_{\mu\nu}(q) = T_{\mu\nu}(q) D_0(q^2)$ , where  $T_{\mu\nu}(q)$  is the transverse projector. The next order terms in Eq. (2) are  $\mathcal{O}(g^3)$ : the contribution involving the four-gluon vertex, and  $\mathcal{O}(g^4)$ : contributions from crossed-box and two-rung gluon ladder diagrams, and 1-loop dressing of the triple-gluon vertex, etc. The color factors in Eqs. (3) and (4) are given by

$$\begin{aligned} t^a t^b t^a = & (C_F - \frac{C_A}{2}) t^b = -\frac{1}{2N_c} t^b \\ t^a f^{abc} t^b = & \frac{C_A}{2} i t^c = \frac{N_c}{2} i t^c \\ t^a t^a = & C_F \mathbf{1}_c = \frac{(N_c^2 - 1)}{2N_c} \mathbf{1}_c. \end{aligned} \quad (5)$$

In contrast, for the color singlet vector vertex, i.e., for the strong dressing of the quark-photon vertex, one has the one-loop Abelian result

$$\begin{aligned} \tilde{\Gamma}_\sigma^{(1)}(p+k, p) = & \tilde{Z}_1 \gamma_\sigma - C_F \int_q^\Lambda g^2 D_{\mu\nu}(p-q) \gamma_\mu S_0(q+k) \\ & \times \gamma_\sigma S_0(q) \gamma_\nu. \end{aligned} \quad (6)$$

To motivate the approximate vertex used in the present study, we note that the local color SU(3) gauge invariance of the QCD action gives the Slavnov-Taylor identity [19] for the gluon vertex

$$\begin{aligned} k_\mu i \Gamma_\mu(p+k, p) = & G(k^2) \{ [1 - B(p, k)] S(p+k)^{-1} \\ & - S(p)^{-1} [1 - B(p, k)] \}, \end{aligned} \quad (7)$$

which relates the divergence of the vertex to the quark propagator  $S(p)$ , the dressing function  $G(k^2)$  of the ghost propagator  $-G(k^2)/k^2$ , and the ghost-quark scattering kernel  $B(p, k)$ , all consistently renormalized. Even though there is no explicit ghost content evident in the 1-loop vertex Eq. (2), it does satisfy this identity at one-loop order [23].

The dressed quark propagator appearing in Eq. (7) is the solution to the gap equation, or the quark Dyson-Schwinger equation, which is

$$S^{-1}(p) = Z_2 S_0^{-1}(p) + C_F Z_1 \int_q^\Lambda g^2 D_{\mu\nu}(p-q) \gamma_\mu \times S(q) \Gamma_\nu(q, p), \quad (8)$$

where  $S_0^{-1}(p) = i\gamma \cdot p + m_{bm}$ ,  $m_{bm}$  is the bare current quark mass, and  $Z_2(\mu^2, \Lambda^2)$  is the quark wave function renormalization constant. The general form for  $S(p)^{-1}$  is

$$S(p)^{-1} = i\gamma \cdot p A(p^2, \mu^2) + B(p^2, \mu^2) \quad (9)$$

and the renormalization condition at scale  $p^2 = \mu^2$  is  $S(p)^{-1} \rightarrow i\gamma \cdot p + m(\mu)$  where  $m(\mu)$  is the renormalized current quark mass.

Prior to the recent appearance of quenched lattice-QCD data [20, 21], there had been little information available on the infrared structure of the gluon-quark vertex. The two  $\mathcal{O}(g^2)$  diagrams of Eq. (2) can not be expected to be adequate there. A common assumption [16] has been to adopt an Abelian vertex Ansatz, such as the Ball-Chiu [17] or Curtis-Pennington [18] forms and attach the appropriate color matrix. In the case of an Abelian U(1) gauge theory, the counterpart to Eq. (7) is the Ward-Takahashi identity (WTI)

$$k_\mu i\tilde{\Gamma}_\mu(p+k, p) = S(p+k)^{-1} - S(p)^{-1}. \quad (10)$$

At  $k = 0$ , the Abelian vertex  $\tilde{\Gamma}_\mu$  has the same general form as given earlier in Eq. (1). The Ward identity  $\tilde{\Gamma}_\sigma(p) = -i\partial S^{-1}(p)/\partial p_\sigma$  yields:  $\tilde{\alpha}_1 = A(p^2)$ ,  $\tilde{\alpha}_2 = 2A'(p^2)$ , and  $\tilde{\alpha}_3 = 2B'(p^2)$ , where  $f' = \partial f(p^2)/\partial p^2$ . However, even if the Abelian Ansatz,  $ig t^c \tilde{\Gamma}_\sigma(p)$ , were to be adopted for the gluon vertex, it would not help in the present context because we need a representation in terms of an explicit set of Feynman diagrams for the resulting self-energy, in order to determine the symmetry-preserving BSE kernel.

In Ref. [12] a study was made of a ladder summation Ansatz for the gluon vertex based on just the Abelian-like gluon exchange diagram of Eq. (3); the symmetry-preserving BSE kernel was generated and used to explore meson and diquark masses. The vertex was generated by iterative and recursive techniques and, after convergence, is equivalent to solution of the integral equation

$$\Gamma_\sigma(p+k, p) = Z_1 \gamma_\sigma - \left(C_F - \frac{C_A}{2}\right) \int_q^\Lambda g^2 D_{\mu\nu}(p-q) \gamma_\mu \times S(q+k) \Gamma_\sigma(q+k, q) S(q) \gamma_\nu. \quad (11)$$

Here, at any order of iteration, the quark propagator is calculated by using the same vertex in the gap equation, Eq. (8). Is this ladder sum a good approximation to the gluon-quark vertex, particularly in the infrared? The quenched lattice-QCD data indicates that the answer is no. The lattice data clearly gives  $\alpha_1(p^2) > 1$  for all available  $p^2$  and the infrared limit appears to be  $\alpha_1(0) \gtrsim 2.2$ . The ladder summation based on Eq. (11) gives  $\alpha_1(p^2) < 1$ , with infrared limit  $\alpha_1(0) \approx 0.94$ . The 1-loop QCD analysis indicates that in the ultra-violet  $\alpha_1(p^2)$  approaches unity from above [23], while the recent model vertex [22], based on a non-perturbative extension of the two 1-loop diagrams from Eq. (2), yields  $\alpha_1(p^2) > 1$  for all  $p^2$ , and agrees quite well with the lattice data.

The reason for this problem can be seen from the color factors associated with the two 1-loop diagrams, Eq. (3) and Eq. (4), which are the leading terms in the ultra-violet region. The ladder sum in Eq. (11) is built on the least significant of the two diagrams; the color factor of the omitted 3-gluon term is  $-N_c^2$  times that of the retained term. The relative contribution to the Slavnov-Taylor identity, Eq. (7), from that term is of the same order at 1-loop. More generally, as discussed in Ref. [14], if  $G(k^2)(1 - B(p, k)) > 0$  persists into the non-perturbative region, one can expect  $\alpha_1(p^2) > 1$ . One can also expect to obtain the wrong sign for  $\alpha_1(p^2) - 1$  if a model kernel has the wrong sign. This is the case with the Abelian-like ladder sum, Eq. (11). Note that in an Abelian  $U(1)$  gauge theory, e.g., the photon-quark vertex,  $\tilde{\alpha}_1(p^2) = A(p^2) > 1$ . An Abelian Ansatz for this amplitude of the gluon-quark vertex might be quite reasonable, but it cannot be simulated by an explicit ladder sum—the color algebra prevents it. In analogy with the photon-quark vertex, where  $\tilde{\alpha}_1(p^2) > 1$  is correlated with the spectral density being positive definite as the timelike region is approached, the gluon-quark vertex dressing has been referred to as an attractive effect in the infrared spacelike region [14]. (Of course, for the gluon vertex there should be no color octet bound states and no positive spectral density in the timelike region.) The 3-gluon coupling is a strong source of the attraction at low spacelike  $p^2$ ; it is  $N_c^2$  times larger than the small repulsive effect of gluon exchange.

Assuming that there is not too much difference in the momentum behavior of the two 1-loop vertex dressing terms in Eq. (2), they were combined in Ref. [14] to write

$$\Gamma_\sigma^{(1)}(p+k, p) \approx Z_1 \gamma_\sigma - \mathcal{C} C_F \int_q^\Lambda g^2 D_{\mu\nu}(p-q) \gamma_\mu S_0(q+k) \times \gamma_\sigma S_0(q) \gamma_\nu, \quad (12)$$

with  $\mathcal{C}$  being an effective color factor. If the momentum dependence of the two combined terms from Eq. (2) was identical, then we see that  $\mathcal{C} = 1$ ; this is equivalent to the Abelian limit. If one were to omit the 3-gluon term altogether, as in the iterative study in Ref. [12], then  $\mathcal{C} = (C_F - \frac{C_A}{2}) C_F^{-1}$ , which for  $N_c = 3$ , gives  $\mathcal{C} = -1/8$ . One

expects that the non-Abelian term is necessary for an effective model and thus that  $0 < \mathcal{C} < 1$ . From Eq. (12), the non-perturbative summation equivalent to the integral equation

$$\Gamma_\sigma(p+k, p) = Z_1 \gamma_\sigma - \mathcal{C} C_F \int_q^\Lambda g^2 D_{\mu\nu}(p-q) \gamma_\mu S(q+k) \times \Gamma_\sigma(q+k, q) S(q) \gamma_\nu, \quad (13)$$

is a natural suggestion. This was studied in Ref. [14], with  $S(q)$  being the self-consistent solution of the quark DSE, Eq. (8), containing the same dressed vertex. A fit to the lattice-QCD data for the vertex gave  $\mathcal{C} = 0.51$ , a value that confirms that attraction by a mechanism outside the scope of iterated gluon exchange is present.

An iterative representation is useful:  $\Gamma_\mu = \sum_{i=0} \Gamma_\mu^i$ , where  $\Gamma_\mu^0 = Z_1 \gamma_\mu$ , and  $i$  labels the number of internal gluon lines. The contribution with  $i+1$  internal gluon lines is obtained from the  $i^{\text{th}}$  contribution by adding one gluon ladder. This is schematically depicted in Fig. 1.

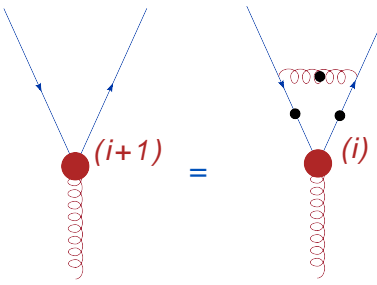


FIG. 1: (Color Online) The iterative relation for successive terms in the ladder-summed vertex. Here the large filled circles denote the dressed quark-gluon vertex, the numbers in the parenthesis denote the numbers of gluon lines contributing to the particular vertices and the small filled circles denote that the propagators are fully dressed. Note that an important non-Abelian term is approximately accounted for by the effective color factor  $\mathcal{C}$  as described in the text.

### A. A wider class of quark-gluon vertex dressing

The enlarged class of dressing diagrams considered in this work is obtained iteratively as depicted in Fig. 2. The contribution with  $i$  internal gluon lines is generated from three contributions having a smaller number of gluon lines by adding one gluon ladder with dressed vertices. If the number of gluon lines in the three vertex contributions are denoted  $j, k$  and  $l$ , then summation is made over  $j, k$  and  $l$  such that  $j+k+l+1 = i$ . Again,

$\Gamma_\mu = \sum_{i=0} \Gamma_\mu^i$ . The iterative scheme is described by

$$\Gamma_\mu^i(p+k, p) = -\mathcal{C} C_F \sum_{\substack{j,k,l \\ i=j+k+l+1}} \int_q^\Lambda g^2 D_{\sigma\nu}(p-q) \times \Gamma_\sigma^j(p+k, q+k) S(q+k) \Gamma_\mu^l(q+k, q) S(q) \Gamma_\nu^k(q, p), \quad (14)$$

for  $i \geq 1$ .

If the iteration is carried to all orders, the equivalent integral equation is

$$\Gamma_\mu(p+k, p) = Z_1 \gamma_\mu - \mathcal{C} C_F \int_q^\Lambda g^2 D_{\sigma\nu}(p-q) \Gamma_\sigma(p+k, q+k) \times S(q+k) \Gamma_\mu(q+k, q) S(q) \Gamma_\nu(q, p). \quad (15)$$

If the iteration is stopped to produce all vertex functions with up to  $n$  internal two point gluon lines, our improved scheme takes into account  $1+n(n+1)(n+2)/6$  diagrams; the corresponding ladder-summed vertex at that order contains a subset of  $(n+1)$  of these diagrams.

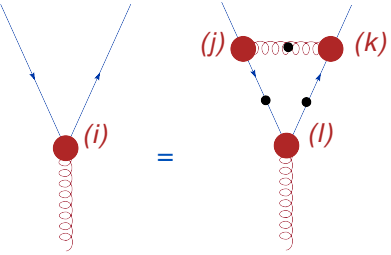


FIG. 2: (Color Online) The iterative relation for the enlarged class of dressing diagrams considered in this work. Here the large filled circles denote the dressed quark-gluon vertex, the numbers in the parenthesis denote the numbers of gluon lines contributing to the particular vertices (with  $j+k+l+1 \equiv i$ ) and the small filled circles denote that the propagators are fully dressed. The vertex contribution with  $i$  internal gluon lines is obtained from vertex contributions with less gluon lines. Note that an important effect of the non-Abelian 3-gluon coupling is approximately accounted for by the effective color factor  $\mathcal{C}$  as described in the text.

In Fig. 3 we use low order diagrams to illustrate the more general class of dressing terms included this way. Note that the included diagrams are restricted to planar diagrams. The contribution from crossed gluon lines in Fig. 3d is not included. All diagrams of the ladder sum used in Ref. [14], such as Fig. 3a, are included; the new element here is the self-consistent dressing of the internal vertices illustrated by Fig. 3b and Fig. 3c.

### B. Symmetry-preserving Bethe-Salpeter kernel

The renormalized homogeneous Bethe-Salpeter equation (BSE) for the quark-antiquark channel, denoted by

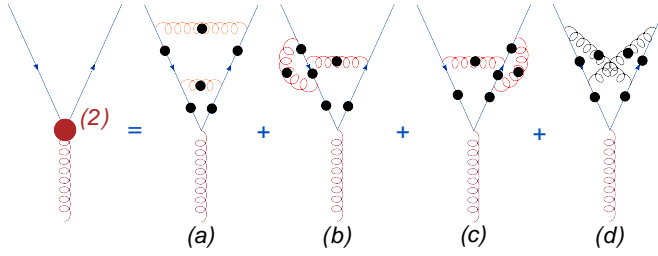


FIG. 3: (Color Online) Vertex skeleton diagrams at  $\mathcal{O}(g^5)$ . Here the large filled circle denotes the quark-gluon vertex dressed to the order of two effective gluon kernel lines. The small filled circles denote that the propagators are fully dressed. Previous work included the ladder structure typified by part (a). The enlarged class of dressing diagrams implemented in this work includes parts (b) and (c) as well. Non-planar diagrams such as part (d) are not accommodated by the present approach. We use an effective color factor to accommodate a major non-Abelian effect from the 3-gluon coupling as described in the text.

$M$ , can be compactly expressed as

$$[\Gamma_M(k; P)]_{EF} = \int_q^\Lambda [K(k, q; P)]_{EF}^{GH} [\chi_M(q; P)]_{GH}, \quad (16)$$

where  $\Gamma_M(k; P)$  is the meson Bethe-Salpeter amplitude (BSA),  $k$  is the relative momentum of the quark-antiquark pair and  $P$  is their total momentum; E,...,H represent color, flavor and spinor indices and the BS wavefunction is

$$\chi_M(k; P) = S(k_+) \Gamma_M(k; P) S(k_-), \quad (17)$$

where  $k_\pm = k \pm \frac{P}{2}$ , and  $K$  is the amputated quark-antiquark scattering kernel. In general the kernel  $K$  is given in terms of the quark self-energy,  $\Sigma$ , by a functional relation dictated by chiral symmetry [10]. This preserves the Ward-Takahashi identity for the color singlet axial vector vertex and ensures that chiral pseudoscalars will remain massless, independent of model details.

In a flavor non-singlet channel, and with equal mass quarks, the axial-vector Ward-Takahashi identity is

$$-iP_\mu \Gamma_\mu^5(p + P, p) = S^{-1}(p + P) \gamma_5 + \gamma_5 S^{-1}(p) - 2m(\mu) \Gamma^5(p + P, p), \quad (18)$$

where we have factored out the explicit flavor matrix. The color-singlet quantities  $\Gamma_\mu^5$  and  $\Gamma^5$  are the axial-vector vertex and the pseudoscalar vertex, respectively, and  $P$  is the total momentum. The amplitude  $\Gamma_\mu^5(p + P, p)$  has a pseudoscalar meson pole. A consequence is that the meson BSE (16) for the (dominant)  $\gamma_5$  amplitude at  $P^2 = 0$  is equivalent to the chiral limit quark DSE for  $B(p^2)$  and a non-zero value for the latter (DCSB) necessarily produces a massless pseudoscalar bound state [7].

The general relation between the BSE kernel,  $K$ , and the quark self-energy,  $\Sigma$ , can be expressed through the

functional derivative [10]

$$K(x', y'; x, y) = -\frac{\delta}{\delta S(x, y)} \Sigma(x', y'). \quad (19)$$

It is to be understood that this procedure is defined in the presence of a bilocal external source for  $\bar{q}q$  and thus  $S$  and  $\Sigma$  are not translationally invariant until the source is set to zero after the differentiation. An appropriate formulation is the Cornwall-Jackiw-Tomboulis effective action [24]. In this context, the above coordinate space formulation ensures the correct number of independent space-time variables will be manifest. Fourier transformation of that 4-point function to momentum representation produces  $K(p, q; P)$  having the correct momentum flow appropriate to the BSE kernel for total momentum  $P$ .

The constructive scheme of Ref. [11] is an example of this relation as applied order by order to a Feynman diagram expansion for  $\Sigma(p)$ . An internal quark propagator  $S(q)$  is removed and the momentum flow is adjusted to account for injection of momentum  $P$  at that point. The number of such contributions coming from one self-energy diagram is the number of internal quark propagators. Hence the rainbow self-energy generates the ladder BSE kernel. A 2-loop self-energy diagram (i.e., from 1-loop vertex dressing) generates 3 terms for the BSE kernel. One can confirm that the axial-vector Ward-Takahashi identity is preserved. Similarly, the vector Ward-Takahashi identity is also preserved.

To be more specific, with the discrete indices made explicit, we apply

$$K_{EF}^{GH} = -\frac{\delta \Sigma_{EF}}{\delta S_{GH}}, \quad (20)$$

to the self-energy given by the second term on the RHS of Eq. (8). After a decomposition

$$\Sigma(k) = \sum_{n=0}^{\infty} \Sigma^n(k), \quad (21)$$

according to the number  $n$  of gluon kernels in the vertex defined by

$$\Sigma^n(k) = C_F \int_q^\Lambda g^2 D_{\mu\nu}(k - q) \gamma_\mu S(q) \Gamma_\nu^n(q, k), \quad (22)$$

for  $n \geq 1$ , with

$$\Sigma^0(k) = m_{bm} + C_F \int_q^\Lambda g^2 D_{\mu\nu}(k - q) \gamma_\mu S(q) \gamma_\nu, \quad (23)$$

The order  $n$  contribution to the BSE kernel is

$$\begin{aligned} [K^n(k, q; P)]_{EF}^{GH} = & -C_F g^2 D_{\mu\nu}(k - q) [\gamma_\mu]_{EG} [\Gamma_\nu^n(q_-, k_-)]_{HF} \\ & - C_F \int_l^\Lambda g^2 D_{\mu\nu}(k - l) [\gamma_\mu S(l_+)]_{EL} \\ & \times \frac{\delta}{\delta S_{GH}(q_\pm)} [\Gamma_\nu^n(l_-, k_-)]_{LF}. \end{aligned} \quad (24)$$

This format is the same as used in Refs. [12] and [14], except that here the content of  $\Gamma_\nu^n$  is more extensive. With a bare vertex the first term of Eq. (24) produces the ladder kernel and the second term is zero. With a vertex up to 1-loop ( $n = 1$ ), the first term of Eq. (24) produces the ladder term plus a 1-loop correction to one vertex; the second term produces two terms: a 1-loop correction to the other vertex and a non-planar term corresponding to crossed gluon lines. These three corrections to the ladder kernel have the same structure as the kernels shown in parts (b), (c), and (d) of Fig. 3. At higher order,  $n > 1$ , the BSE kernel produced in the present work departs from that considered in Ref. [14].

After substitution of Eq. (24) into the BSE Eq. (16), and with a change of variables, the meson BSE becomes

$$\Gamma_M(k; P) = -C_F \int_q^\Lambda g^2 D_{\mu\nu}(k - q) \gamma_\mu \times [\chi_M(q; P) \Gamma_\nu(q_-, k_-) + S(q_+) \Lambda_{M\nu}(q, k; P)], \quad (25)$$

where we denote by  $\Lambda_{M\nu}$  the summation to all orders of the functional derivative of the vertex as indicated in Eq. (24). In particular,

$$\Lambda_{M\nu}(q, k; P) = \sum_{n=0}^{\infty} \Lambda_{M\nu}^n(q, k; P), \quad (26)$$

with

$$[\Lambda_{M\nu}^n(q, k; P)]_{LF} = \int_l^\Lambda \frac{\delta}{\delta S_{GH}(l_\pm)} [\Gamma_\nu^n(q_-, k_-)]_{LF} \times [\chi_M(l; P)]_{GH}. \quad (27)$$

The vertex iteration given in Eq. (14) produces the recurrence formula for the  $\Lambda_{M\nu}^n$

$$\begin{aligned} \Lambda_{M\nu}^n(q, k; P) &= -CC_F \sum_{\substack{j, k, h \\ n=j+k+h+1}} \left[ \int_t^\Lambda g^2 D_{\rho\sigma}(q - t) \Gamma_\rho^j(q_+, t_+) \chi_M(t; P) \Gamma_\nu^k(t_-, t_- + k - q) \right. \\ &\quad \times S(t_- + k - q) \Gamma_\sigma^h(t_- + k - q, k_-) \\ &\quad + \int_t^\Lambda g^2 D_{\rho\sigma}(k - t) \Gamma_\rho^j(q_+, t_+ + q - k) S(t_+ + q - k) \\ &\quad \times \Gamma_\nu^k(t_+ + q - k, t_+) \chi_M(t; P) \Gamma_\sigma^h(t_-, k_-) \\ &\quad + \int_t^\Lambda g^2 D_{\rho\sigma}(q - t) \Lambda_{M\rho}^j(q, t; P) S(t_-) \Gamma_\nu^k(t_-, t_- + k - q) \\ &\quad \times S(t_- + k - q) \Gamma_\sigma^h(t_- + k - q, k_-) \\ &\quad + \int_t^\Lambda g^2 D_{\rho\sigma}(q - t) \Gamma_\rho^j(q_+, t_+) S(t_+) \Lambda_{M\nu}^k(t, t + k - q; P) \\ &\quad \times S(t_- + k - q) \Gamma_\sigma^h(t_- + k - q, k_-) \\ &\quad \left. + \int_t^\Lambda g^2 D_{\rho\sigma}(q - t) \Gamma_\rho^j(q_+, t_+) S(t_+) \Gamma_\nu^k(t_+, t_+ + k - q) \right. \\ &\quad \times S(t_+ + k - q) \Lambda_{M\sigma}^h(t + k - q, k; P) \end{aligned} \quad (28)$$

where  $\Lambda_{M\nu}^0(q, k; P) = 0$ .

The structure of the  $q\bar{q}$  BS kernel produced by Eq. (25) and Eq. (28) is schematically depicted in Figs. 4 and 5.

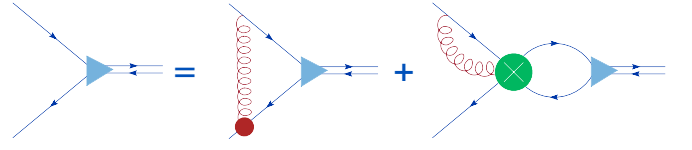


FIG. 4: (Color Online) Kernel decomposition. The filled triangles represent the meson BSAs, the filled circle represents the dressed quark-gluon vertex and the crossed circle represents the  $\Lambda$  function.

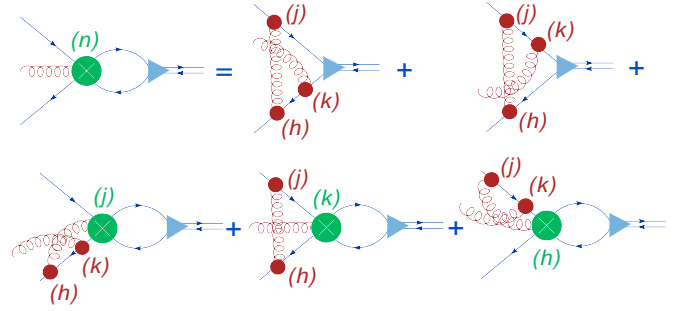


FIG. 5: (Color Online)  $\Lambda$  function decomposition. The filled triangles represent the meson BSAs, the filled circles represent the dressed quark-gluon vertices and the crossed circles represent the  $\Lambda$  functions. The numbers in the parenthesis denote the numbers of gluon lines contributing to the particular functions.

With a general interaction kernel,  $g^2 D_{\rho\sigma}$ , it is exceedingly difficult to implement this formal recurrence relation to obtain a BS kernel because of overlapping multiple integrals that compound rapidly with increasing order.

### III. ALGEBRAIC ANALYSIS

#### A. The interaction model

In the ultraviolet, the kernel of the quark DSE, Eq. (8), takes the form

$$Z_1 \gamma_\mu g^2 D_{\mu\nu}(k) \Gamma_\nu(q, p) \rightarrow 4\pi\alpha(k^2) \gamma_\mu D_{\mu\nu}^{\text{free}}(k) \gamma_\nu, \quad (29)$$

where  $k = p - q$ , and  $\alpha(k^2)$  is the renormalized strong running coupling, which has absorbed the renormalization constants of the quark and gluon propagators and the vertex. The ladder-rainbow truncations that have been phenomenologically successful in recent years for light quark hadrons adopt the form of Eq. (29) for all  $k^2$  by replacing  $\alpha(k^2)$  by  $\alpha_{\text{eff}}(k^2)$ , which contains the correct 1-loop QCD ultra-violet form and a parameterized infrared behavior fitted to one or more chiral observables such as  $\langle \bar{q}q \rangle_\mu^0$ . In this sense, such an  $\alpha_{\text{eff}}(k^2)$  contains those infrared effects of the dressed vertex  $\Gamma_\nu(q, p)$  that can be mapped into a single effective amplitude corresponding to  $\gamma_\nu$  for chiral quarks. Such a kernel does not

have the explicit dependence upon quark mass that would occur if the vertex dressing were to be generated by an explicit Feynman diagram structure. In particular, one expects the vertex dressing to decrease with increasing quark mass; the effective ladder-rainbow kernel appropriate to heavy quark hadrons should have less infrared strength from dressing than is the case for light quark hadrons.

We use an explicit (but approximate) diagrammatic description of the dressed vertex  $\Gamma_\nu(q, p)$ , and to facilitate the analysis we make the replacement  $4\pi\alpha_{\text{eff}}(k^2)/k^2 \rightarrow (2\pi)^4\mathcal{G}^2\delta^4(k)$ . This is the Munczek-Nemirovsky Ansatz [15] for the interaction kernel. The parameter  $\mathcal{G}^2$  is a measure of the integrated kernel strength, and we expect this to be less than what would be necessary in ladder-rainbow format because of the infrared structure now to be provided explicitly by the model vertex  $\Gamma_\mu(q, p)$ . The equations of the previous Sections convert to model form by the replacement

$$g^2 D_{\mu\nu}(k) \rightarrow \left( \delta_{\mu\nu} - \frac{k_\mu k_\nu}{k^2} \right) (2\pi)^4 \mathcal{G}^2 \delta^4(k), \quad (30)$$

where we choose Landau gauge. It is the combination of Eq. (30) and the model vertex that is the DSE kernel; comparisons of Eq. (30) with information about the dressed gluon 2-point function are incomplete. The resulting DSEs for the quark propagator and gluon-quark vertex are ultra-violet finite; thus the renormalization constants are unity:  $Z_1 = Z_2 = 1$ , and there is no distinction between bare and renormalized quark current mass. We set  $m_{bm} = m(\mu) = m$ .

## B. The algebraic vertex and quark propagator

With this kernel, the vertex integral equation Eq. (15) determines solutions for  $k = 0$  and we define  $\Gamma_\mu(p, p) := \Gamma_\mu(p)$ . The resulting algebraic form for Eq. (15) is

$$\Gamma_\mu(p) = \gamma_\mu - \mathcal{C}\mathcal{G}^2\Gamma_\sigma(p)S(p)\Gamma_\mu(p)S(p)\Gamma_\sigma(p). \quad (31)$$

In obtaining this form, we have used  $3C_F/4 = 1$ , where the extra factor of  $3/4$  arises from the transverse projector. The general form of the vertex is:

$$\begin{aligned} \Gamma_\mu(p) = & \alpha_1(p^2)\gamma_\mu + \alpha_2(p^2)\gamma \cdot p p_\mu - \alpha_3(p^2)ip_\mu \\ & + \alpha_4(p^2)i\gamma_\mu \gamma \cdot p \end{aligned} \quad (32)$$

where  $\alpha_i(p^2)$  are invariant amplitudes. From Eq. (31) we find  $\alpha_4 = 0$ , as was the case for the related models in Refs. [12] and [14].

The vertex is a sum over contributions with exactly  $n$  internal effective gluon kernels according to

$$\Gamma_\mu(p) = \sum_{n=0}^{\infty} \Gamma_\mu^n(p), \quad (33)$$

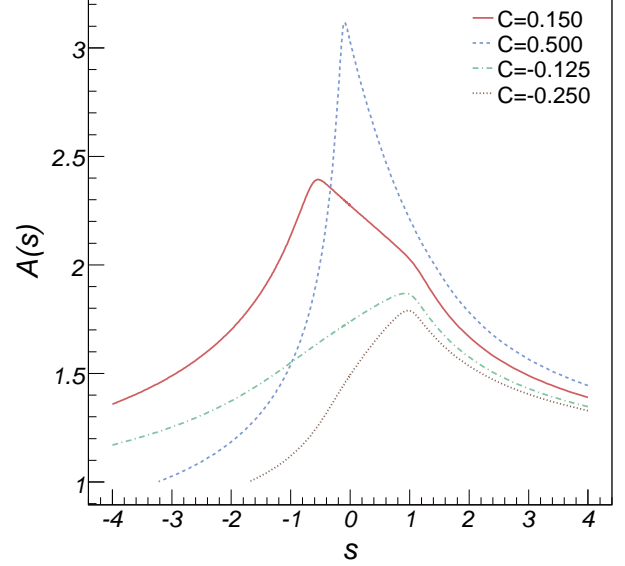


FIG. 6: (Color Online) Quark propagator amplitude  $A(s)$  versus Euclidean  $s = p^2$ . We use the interaction mass scale  $\mathcal{G} = 1$  GeV and the current mass is  $m = 0.0183$   $\mathcal{G} = 18.3$  MeV.  $\mathcal{C}$  dependence calculated with converged summation of vertex dressing, for  $\mathcal{C} = 0.15$  (solid curve),  $\mathcal{C} = 0.5$  (dashed curve),  $\mathcal{C} = -0.125$  (dot-dashed curve) and  $\mathcal{C} = -0.25$  (dotted curve).

with the general contribution given by the recursive relation

$$\Gamma_\mu^n(p) = -\mathcal{C}\mathcal{G}^2 \sum_{\substack{j,k,l \\ n=j+k+l+1}} \Gamma_\nu^j(p)S(p)\Gamma_\mu^k(p)S(p)\Gamma_\nu^l(p), \quad (34)$$

where  $\Gamma_\mu^0(p) = \gamma_\mu$ . Substitution of the form  $S(p)^{-1} = i\gamma \cdot p A(p^2) + B(p^2)$  into Eq.(34) gives  $\Gamma_\mu^n(p^2)$  in terms of the functions  $A(p^2)$  and  $B(p^2)$ . These latter functions must be solved simultaneously with the vertex at the given order. The algebraic form of the gap equation for the propagator is

$$S^{-1}(p) = i\gamma \cdot p + m + \mathcal{G}^2\gamma_\mu S(p)\Gamma_\mu(p), \quad (35)$$

where again the transverse projector and the color factor combine to yield  $3C_F/4 = 1$ . After projection onto the two Dirac amplitudes we have

$$A(p^2) = 1 - \mathcal{G}^2 \frac{i}{4} \text{tr} \left[ \frac{\gamma \cdot p}{p^2} \gamma_\mu S(p) \Gamma_\mu(p) \right], \quad (36)$$

$$B(p^2) = m + \mathcal{G}^2 \frac{1}{4} \text{tr} [\gamma_\mu S(p) \Gamma_\mu(p)]. \quad (37)$$

Equations (34), (36) and (37) are solved simultaneously at a specified order  $n$  of vertex dressing.

In the case where one is limited to a strict ladder summation for the vertex with bare internal vertices, closed

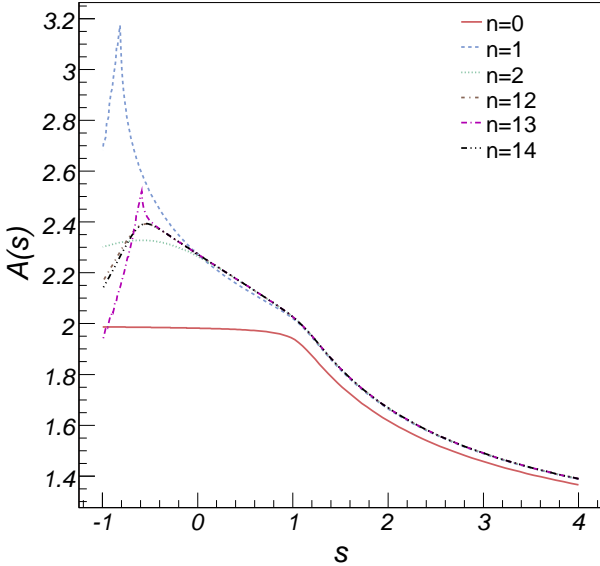


FIG. 7: (Color Online) Quark propagator amplitude  $A(s)$  versus Euclidean  $s = p^2$ . We use the interaction mass scale  $\mathcal{G} = 1$  GeV and the current mass is  $m = 0.0183$   $\mathcal{G} = 18.3$  MeV. We show the influence of vertex dressing to order  $n$  as described in the text. For  $\mathcal{C} = 0.15$ ,  $n = 0$  yields the solid curve and the result is the ladder-rainbow truncation. The other curves are  $n = 1$  (long dashed curve, 1-loop vertex),  $n = 2$  (dotted curve, 2-loop vertex),  $n = 12$  (dot - short dashed curve),  $n = 13$  (dot - long dashed curve) and  $n = 14$  (dot dot dot - dashed curve) order of dressing of the quark gluon vertex.

form expressions for the vertex amplitudes  $\alpha_i$  in terms of  $A$  and  $B$  are obtainable [12, 14]. With the enlarged class of dressing considered here, corresponding closed form expressions have not been obtained. However numerical evaluation is sufficient for the vertex and propagator amplitudes; a numerical treatment of the BSE kernel must be made in any case. Numerical solution of the simultaneous algebraic equations for the vertex and propagator is carried out here using the algebraic and numerical tools of *Mathematica* [25] with the assistance of the *FeynCalc* package used for computer-algebraic evaluation of the Dirac algebra [26].

The model parameter  $\mathcal{C}$  for the vertex is determined by a fit to selected global features of quenched lattice-QCD data for the quark propagator [27] and the quark-gluon vertex [20]. This data is available for both quantities at current quark mass  $m = \bar{m} = 60$  MeV. This is the same data as used to fit the same parameter  $\mathcal{C}$  in Ref. [14]; a different result will therefore reflect the wider class of vertex dressing herein. To facilitate comparison we also eliminate the role of the interaction strength mass scale parameter  $\mathcal{G}$  in this step by dealing with dimensionless quantities;  $\mathcal{G}$  will later be fixed by requiring that  $m_\rho$  be reproduced.

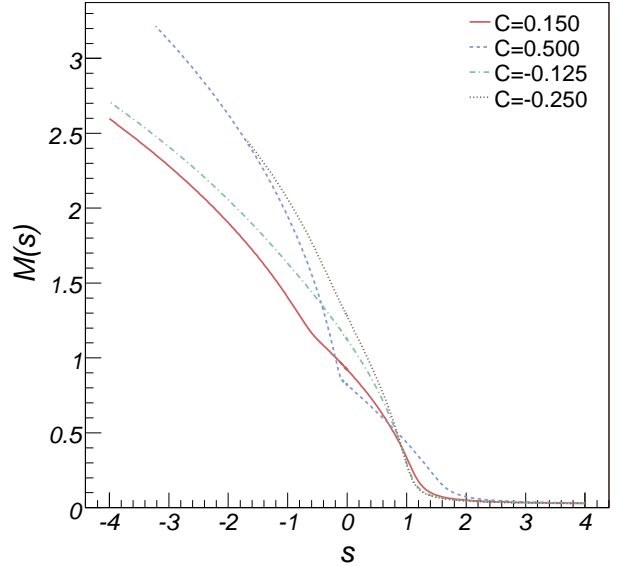


FIG. 8: (Color Online) Quark mass function  $M(s)$  versus Euclidean  $s = p^2$ . We use the interaction mass scale  $\mathcal{G} = 1$  GeV and the current mass is  $m = 0.0183$   $\mathcal{G} = 18.3$  MeV.  $\mathcal{C}$  dependence calculated with converged summation of vertex dressing, for  $\mathcal{C} = 0.15$  (solid curve),  $\mathcal{C} = 0.5$  (dashed curve),  $\mathcal{C} = -0.125$  (dot-dash curve) and  $\mathcal{C} = -0.25$  (dotted curve).

The lattice-QCD data for the quark propagator indicates that  $Z_{qu}(0) \equiv 1/A_{qu}(0) \approx 0.7$  and  $M_{qu}(0) \equiv B(0)/A(0) \approx 0.42$  GeV. Following Ref. [14] the lattice data for both the propagator and the vertex in the infrared is characterized by the set of four dimensionless quantities evaluated at  $p^2 = 0$ :

$$A(0, m_{60}) = 1.4 \quad (38)$$

$$\alpha_1(0, m_{60}) = 2.1 \quad (39)$$

$$-M(0, m_{60})^2 \alpha_2(0, m_{60}) = 7.1 \quad (40)$$

$$-M(0, m_{60}) \alpha_3(0, m_{60}) = 1.0, \quad (41)$$

where  $m_{60} = \bar{m}/M_{qu}(0)$ . The best fit to these quantities gives  $\mathcal{C} = 0.34$  with an average relative error of  $\bar{r} = 24\%$  and standard deviation  $\sigma_r = 70\%$ . The quality of fit is about the same as in Ref. [14], and changes  $\Delta\mathcal{C} \approx \pm 0.2$  are not significant in this regard. For example,  $\mathcal{C} = 0.15$  leads to  $\bar{r} = 39\%$  and  $\sigma_r = 72\%$ . We will use  $\mathcal{C} = 0.15$  because the resulting vertex at timelike  $p^2$  is more convergent with respect to increasing order of dressing. The value of  $\mathcal{C}$  being significantly greater than the

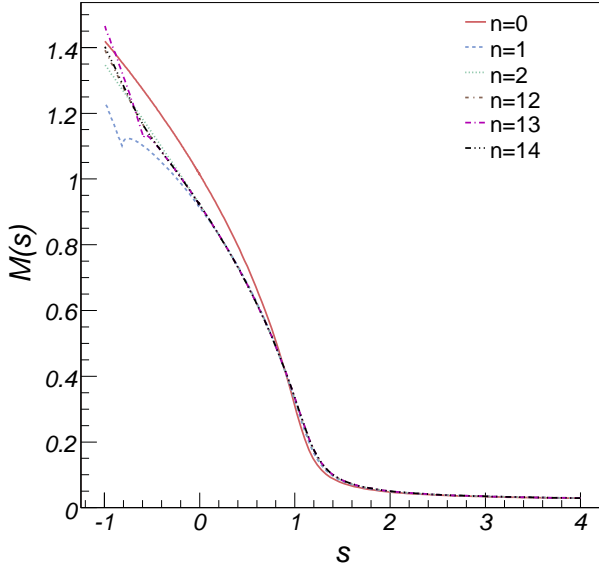


FIG. 9: (Color Online) Quark mass function  $M(s)$  versus Euclidean  $s = p^2$ . We use the interaction mass scale  $\mathcal{G} = 1$  GeV and the current mass is  $m = 0.0183 \mathcal{G} = 18.3$  MeV. We show the influence of vertex dressing to order  $n$  as described in the text. For  $\mathcal{C} = 0.15$ ,  $n = 0$  yields the solid curve and the result is the ladder-rainbow truncation. The other curves are  $n = 1$  (long dashed curve, 1-loop vertex),  $n = 2$  (dotted curve, 2-loop vertex),  $n = 12$  (dot-short dashed curve),  $n = 13$  (dot-long dashed curve) and  $n = 14$  (dot-dot-dot-dashed curve) order of dressing of quark gluon vertex.

strict ladder sum limit  $\mathcal{C} = -1/8$ , we see that the attraction provided by the 3-gluon coupling is important for the vertex. However the amount of attraction that must be provided in this phenomenological way in the present work is less than what was required in Ref. [14] to fit the same lattice quantities. In that work,  $\mathcal{C} = 0.51$  was found necessary. We attribute this difference to the fact that a wider class of self-consistent dressing diagrams is included in the present approach; attraction is provided by every vertex that is internal in the sense of Fig. 2.

In Figs. 6 and 7 we present the results for our calculations of  $A(p^2)$  for different values of  $\mathcal{C}$  and different orders of quark-gluon vertex dressing. We set  $\mathcal{G} = 1$  GeV, so all dimensioned quantities are measured in units of  $\mathcal{G}$ . The current mass is  $m_q = 0.0183 \mathcal{G}$ . One can see from Fig. 6 that  $\mathcal{C}$  has a major impact on the behavior of  $A(s)$ , especially in the timelike region. Fig. 7 shows that with  $n = 14$  as the order of dressing of the quark-gluon vertex, we achieved convergence of the quark propagator function  $A(p^2)$  for  $p^2 > -\mathcal{G}^2$ . The same is true for the function  $B(p^2)$ . The relative measure of the convergence of the quark propagator functions with  $n$  is the convergence of the meson masses calculated using the solutions for the propagators. It will be shown later on that our

calculations of  $m_\pi$  and  $m_\rho$  have converged to better than 1% for  $n = 14$ . For heavier current quarks the convergence region for the solutions of  $A(p^2)$  and  $B(p^2)$  extends deeper into the time-like region of  $p^2$ , which allows for convergent calculations of heavier meson masses.

In Figs. 8 and 9 we present the results for our calculations of  $M(p^2) = B(p^2)/A(p^2)$  for different values of  $\mathcal{C}$  and different orders of quark-gluon vertex dressing. Again these calculations have  $\mathcal{G} = 1$  GeV, so all dimensioned quantities are measured in units of  $\mathcal{G}$ . The vertex parameter  $\mathcal{C}$  has a modest impact on the behavior of  $M(s)$ .

Figs. 10, 11 and 12 display the results for the vertex amplitudes  $\alpha_i(s)$  corresponding to different orders of vertex dressing. Successive orders after 1-loop ( $n = 1$ ) serve to enhance the infrared strength for  $s < 1$ . The convergence with  $n$  is monotonic, in contrast to the convergence of the BSE kernel that is generated from this vertex, as discussed later.

The quark condensate in the present model is given by

$$\langle \bar{q}q \rangle^0 = -\frac{3}{4\pi^2} \int_0^{s_0} ds s \frac{B_0(s)}{s A_0^2(s) + B_0^2(s)}, \quad (42)$$

in terms of the chiral limit quark propagator amplitudes. There is no renormalization necessary because there is a spacelike  $s_0$  for which  $B_0(s > s_0) = 0$ . Because of the underrepresentation of the ultra-violet strength of the interaction in this model, the condensate is characteristically too low. In particular we find

$$-\langle \bar{q}q \rangle_{\mathcal{C}=0.15}^0 = (0.2146 \mathcal{G})^3 = (0.1266 \text{ GeV})^3 \quad (43)$$

with  $\mathcal{G} = 0.59$  GeV. The rainbow-ladder result ( $\mathcal{C} = 0$ ) is  $-\langle \bar{q}q \rangle_{\text{LR}}^0 = \mathcal{G}^3/(10\pi^2) = (0.1277 \text{ GeV})^3$ . Thus one can see that the vertex dressing decreases the condensate slightly. In more detail, we have

$$\frac{\langle \bar{q}q \rangle_{\text{LR}}^0}{\langle \bar{q}q \rangle_{\mathcal{C}=0.15}^0} = 1.03, \quad (44)$$

which indicates that the ladder-rainbow truncation overestimates the condensate by 3% compared to the more completely dressed vertex considered here. The previous study [14] with a more restricted class of vertex dressing diagrams found that the ladder-rainbow truncation was 18% too low.

### C. The algebraic Bethe-Salpeter kernel for mesons

Substitution of the model interaction kernel Eq. (30) into the meson BSE, Eq. (25), produces the algebraic form

$$\begin{aligned} \Gamma_M(k; P) = & -\mathcal{G}^2 \gamma_\mu \{ \chi_M(k; P) \Gamma_\mu(k_-) \\ & + S(k_+) \Lambda_{M\mu}(k; P) \}. \end{aligned} \quad (45)$$

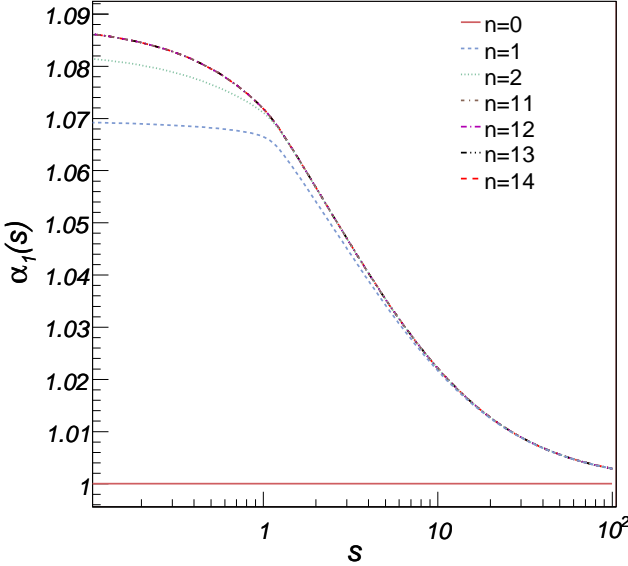


FIG. 10: (Color Online) Gluon-quark vertex amplitude  $\alpha_1(s)$  versus Euclidean  $s = p^2$ , for  $\mathcal{C} = 0.15$ . We use the interaction mass scale  $\mathcal{G} = 1$  GeV and the current mass is  $m = 0.0183$   $\mathcal{G} = 18.3$  MeV.  $n = 0$  (solid curve) results from the bare vertex and is the ladder-rainbow truncation. The other curves are  $n = 1$  (short dashed curve, 1-loop vertex dressing),  $n = 2$  (dotted curve),  $n = 11$  (dot - short dashed curve),  $n = 12$  (dot - long dashed curve),  $n = 13$  (dot dot dot - dashed curve) and  $n = 14$  (long dashed curve).

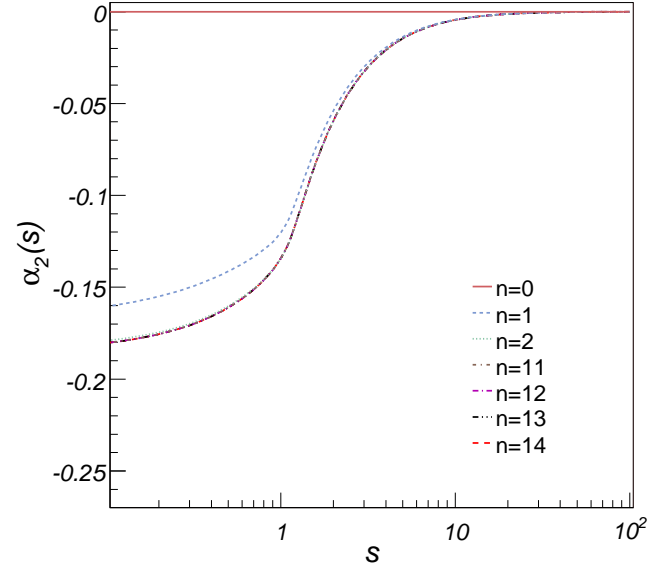


FIG. 11: (Color Online) Gluon-quark vertex amplitude  $\alpha_2(s)$  versus Euclidean  $s = p^2$ , for  $\mathcal{C} = 0.15$ . We use the interaction mass scale  $\mathcal{G} = 1$  GeV and the current mass is  $m = 0.0183$   $\mathcal{G} = 18.3$  MeV.  $n = 0$  (solid curve) results from the bare vertex and is the ladder-rainbow truncation. The other curves are  $n = 1$  (short dashed curve, 1-loop vertex dressing),  $n = 2$  (dotted curve),  $n = 11$  (dot - short dashed curve),  $n = 12$  (dot - long dashed curve),  $n = 13$  (dot dot dot - dashed curve) and  $n = 14$  (long dashed curve).

The previous general recurrence relation Eq. (28) for the general term of  $\Lambda_{M\nu} = \sum_{n=0}^{\infty} \Lambda_{M\nu}^n$  now has the algebraic form

$$\begin{aligned} \Lambda_{M\nu}^n(k; P) = & -\mathcal{C}\mathcal{G}^2 \sum_{\substack{j,k,h \\ n=j+k+h+1}} \\ & [\Gamma_\rho^j(k_+) \chi_M(k; P) \Gamma_\nu^k(k_-) S(k_-) \Gamma_\rho^h(k_-) \\ & + \Gamma_\rho^j(k_+) S(k_+) \Gamma_\nu^k(k) \chi_M(k; P) \Gamma_\rho^h(k_-) \\ & + \Lambda_{M\rho}^j(k; P) S(k_-) l^a \Gamma_\nu^k(k_-) S(k_-) \Gamma_\sigma^h(k_-) \\ & + \Gamma_\rho^j(k_+) S(q_+) \Lambda_{M\nu}^k(k; P) S(k_-) \Gamma_\rho^h(k_-) \\ & + \Gamma_\rho^j(k_+) S(k_+) \Gamma_\nu^k(k_+) S(k_+) \Lambda_{M\sigma}^h(k; P)]. \end{aligned} \quad (46)$$

If we work at a given order,  $n$ , of vertex dressing, then the quark propagator, the dressed vertex, and the BSE kernel can be constructed recursively. By construction, chiral symmetry is preserved and the chiral pseudoscalar states are massless, independent of model parameters. Because of the algebraic structure, in which the BS amplitude  $\Gamma_M(k; P)$  appears on both sides of Eq. (45) with the same  $q\bar{q}$  relative momentum  $k$ , a physical solution where  $P^2 = -M_M^2$  is independent of  $k$  is defined only at  $k = 0$ . That is, the quark and antiquark have momenta  $\eta P$  and  $(1 - \eta)P$ . (Here we consider only equal mass

quarks and thus have chosen  $\eta = 1/2$ .) The Munczek-Nemirovsky model interaction does not allow momentum transfer to quarks. This is a restriction present in all hadron studies made within this model. We define  $\Gamma_M(P) = \Gamma_M(k = 0; P)$ , after which the form in which we solve the BSE is

$$\begin{aligned} \Gamma_M(P) = & -\mathcal{G}^2 \gamma_\mu S\left(\frac{P}{2}\right) \left\{ \Gamma_M(P) S\left(-\frac{P}{2}\right) \Gamma_\mu\left(-\frac{P}{2}\right) \right. \\ & \left. + \Lambda_{M\mu}(0; P) \right\}. \end{aligned} \quad (47)$$

#### IV. MESON MASSES AND RESULTS

The general form of a meson BS amplitude can be written as

$$\Gamma_M(k; P) = \sum_i \mathcal{K}^i(k; P) f_M^i(k^2, k \cdot P; P^2), \quad (48)$$

where the  $\mathcal{K}^i(k; P)$  are a complete set of independent covariants constructed from Dirac matrices and momenta that transform in a manner specified by the quantum numbers of the meson under consideration. The  $f_M^i(k^2, k \cdot P; P^2)$  are the corresponding invariant amplitudes. (We do not show explicitly the color singlet

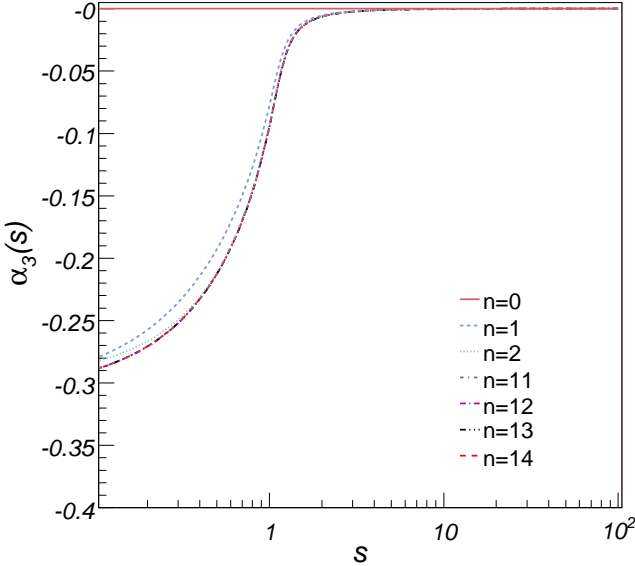


FIG. 12: (Color Online) Gluon-quark vertex amplitude  $\alpha_3(s)$  versus Euclidean  $s = p^2$ , for  $\mathcal{C} = 0.15$ . We use the interaction mass scale  $\mathcal{G} = 1$  GeV and the current mass is  $m = 0.0183 \mathcal{G} = 18.3$  MeV.  $n = 0$  (solid curve) results from the bare vertex and is the ladder-rainbow truncation. The other curves are  $n = 1$  (short dashed curve, 1-loop vertex dressing),  $n = 2$  (dotted curve),  $n = 11$  (dot - short dashed curve),  $n = 12$  (dot - long dashed curve),  $n = 13$  (dot dot dot - dashed curve) and  $n = 14$  (long dashed curve).

unit matrix.) The model BSE under consideration here, Eq. (47), has relative momentum  $k = 0$ , and the set of covariants is reduced considerably. We have

$$\Gamma_M(P) = \sum_{i=1}^N \mathcal{K}^i(P) f_M^i(P^2) \quad (49)$$

and it is convenient to develop a set of projection operators  $\mathcal{P}_j$  that allow us to isolate each amplitude according to

$$f_M^j = \text{Tr}_D [\mathcal{P}_j \Gamma_M]. \quad (50)$$

Then projection of the BSE, Eq. (47), yields the eigenvalue equation

$$f(P^2) = \mathcal{H}(P^2) f(P^2), \quad (51)$$

where  $f = (f_M^1, f_M^2, \dots)$  is a vector of invariant amplitudes and the matrix  $\mathcal{H}(P^2)$  is an  $N \times N$  representation of the kernel.

The mass,  $M_M$ , of the lowest bound state is obtained from the highest negative value of  $P^2$  for which

$$\det [\mathcal{H}(P^2) - I]_{P^2+M_M^2=0} = 0. \quad (52)$$

This method, namely the solution of the characteristic polynomial for Eq. (51), has also been followed in earlier work of this type [12, 14].

### A. The Pion

The general form of the  $\pi$  Bethe-Salpeter amplitude requires four covariants and is

$$\Gamma_\pi(k; P) = \gamma_5 [i f_\pi^1 + \gamma \cdot P f_\pi^2 + \gamma \cdot k k \cdot P f_\pi^3 + \sigma_{\mu\nu} k_\mu P_\nu f_\pi^4], \quad (53)$$

in terms of amplitudes  $f_\pi^i(k^2, k \cdot P; P^2)$ . We do not show flavor dependence since we treat u-quarks and d-quarks the same in all other respects. In the present case only two covariants survive and we have

$$\Gamma_\pi(P) = \gamma_5 [i f_\pi^1(P^2) + \gamma \cdot P f_\pi^2(P^2)]. \quad (54)$$

Convenient projection operators in this case are

$$\mathcal{P}_1 = -\frac{i}{4} \gamma_5, \quad \mathcal{P}_2 = \frac{1}{4P^2} \gamma \cdot P \gamma_5. \quad (55)$$

### B. The Rho

The general form of the  $\rho$  Bethe-Salpeter amplitude requires eight transverse covariants and corresponding amplitudes. Specific choices that have been found convenient in earlier work are given in Refs. [5, 28]. In the present case, the most general form is simply

$$\Gamma_{\rho\mu}(P) = \left( \delta_{\mu\nu} - \frac{P_\mu P_\nu}{P^2} \right) \gamma_\nu f_\rho^1(P^2) + \sigma_{\mu\nu} P_\nu f_\rho^2(P^2). \quad (56)$$

Again a unit color matrix is understood and we treat u-quarks and d-quarks as the same. Convenient projection operators that isolate the amplitudes are

$$\mathcal{P}_1 = \frac{1}{12} \gamma_\mu, \quad \mathcal{P}_2 = \frac{1}{12P^2} \sigma_{\mu\nu} P_\nu. \quad (57)$$

### C. Vertex Dressing for Light Quarks

There are a total of three parameters:  $\mathcal{C} = 0.15$ , which has already been set by the quenched lattice data for the quark propagator and the gluon-quark vertex, while the experimental  $m_\pi$  and  $m_\rho$  are used to set the other two: the interaction mass scale,  $\mathcal{G} = 0.59$  GeV, and the current mass for the u/d quark,  $m = 0.0183 \mathcal{G} = 11$  MeV. The fully dressed vertex model is used in these determinations. In practice, we require convergence to 3 significant figures for the masses and this is achieved with a vertex dressed to order  $n = 14$ . Table I shows how the vertex dressing influences  $m_\pi$  and  $m_\rho$ .

To confirm that our constructed BSE kernel preserves chiral symmetry, we verified that to any order of vertex dressing, and with  $m = 0$ , the chiral pion is massless to the numerical accuracy considered. The physical  $m_\pi$  is not fixed perfectly by the symmetry but is almost so. The explicit symmetry breaking by the current mass is sufficient to determine  $m_\pi$  for all orders of vertex dressing

TABLE I: Effect of quark-gluon vertex dressing to order  $n$  upon the masses of the  $\pi$  and  $\rho$  mesons (in GeV). The ladder-rainbow (LR) truncation corresponds to  $n = 0$ , one loop vertex dressing corresponds to  $n = 1$ , etc, while the full model result (converged to 3 significant figures) is labeled  $n = \infty$ . Also displayed for  $m_\rho$  is the mass error,  $\Delta m_\rho$ , and the relative mass error,  $\Delta m_\rho/m_\rho$ , of the LR truncation of the present model compared to a previous model [14] based on a limited class of vertex dressing diagrams. The mass scale parameter is  $\mathcal{G} = 0.59$  GeV, the current mass of the u/d-quark is  $m = 0.0183\mathcal{G} = 11$  MeV, and  $\mathcal{C} = 0.15$ .

Vertex Dressing	$m_\pi$	$m_\rho$	$\Delta m_\rho$	$\frac{\Delta m_\rho}{m_\rho}$	$\frac{\Delta m_\rho}{m_\rho}$ [14]
$n = 0$ (LR)	0.140	0.850	+0.074	+0.095	+0.295
$n = 1$ (1-loop)	0.135	0.759	-0.017	-0.022	—
$n = 2$	0.135	0.781	+0.005	+0.006	+0.096
$n = 3$	0.135	0.772	-0.004	-0.005	N/A
$n = 4$	0.135	0.778	+0.002	+0.003	N/A
$n = \infty$ (full model)	0.135	0.776	0.0	0.0	0.0

except for a few % error in the ladder-rainbow truncation ( $n = 0$ ). Since the same behavior was observed in earlier work of this nature [12, 14], this result is quite model-independent.

The response of  $m_\rho$  to increasing order of vertex dressing shows that the ladder-rainbow truncation is missing 74 MeV of attraction compared to the full model result. The error decreases with each added order of vertex dressing. The relative error in the ladder-rainbow mass is 9.5% in the present vertex model, compared to 29.5% in the vertex model of Ref. [14]. Here each diagram for the dressed vertex has each of its internal vertices dressed in a self-consistent way. There are evidently both attractive and repulsive contributions at the various orders that combine to add less net attraction to the ladder-rainbow truncation than what was found in Ref. [14].

#### D. Current Quark Mass Dependence

One expects the influence of vertex dressing to decrease with increasing quark mass because of the internal quark propagators in the vertex. Thus the LR truncation should become more accurate for mesons involving heavier quarks. It is useful to quantify this for the following reason. Phenomenological LR kernels [3] are capable of incorporating many realistic features of QCD modeling and have been developed to provide efficient descriptions of light quark mesons, their elastic and transition form factors, and decay constants. A parameterized LR kernel that reproduces the experimental  $m_\pi$  and  $m_\rho$  has, by definition, absorbed the effective dressing of the vertex. The present work suggests that this is an amount of vertex attraction worth 9.5% of the vector meson mass. However this phenomenological representation of the dressing does not have an explicit dependence upon quark mass

TABLE II: Error of the ladder-rainbow truncation for equal quark mass vector mesons in the u/d-, s-, c-, and b-quark regions, according to calculated mass and effective binding energies (in GeV). The ladder-rainbow (LR) truncation corresponds to order  $n = 0$  in vertex dressing and the full model result corresponds to vertex dressing to all orders,  $n = \infty$ , in this model. The mass scale parameter is  $\mathcal{G} = 0.59$  GeV, and  $\mathcal{C} = 0.15$ .

	ladder-rainbow	full model	LR % error	
	$n = 0$	$n = \infty$	this model	[14]
$m_{u,d} = 0.011$				
$m_\rho$	0.850	0.776	9.5%	30%
$\mathcal{BE}_\rho$	0.346	0.311	11%	
$m_s = 0.165$				
$m_\phi$	1.08	1.02	6.0%	21%
$\mathcal{BE}_\phi$	0.350	0.320	9.0%	
$m_c = 1.35$				
$m_{J/\psi}$	3.11	3.09	0.3%	3.5%
$\mathcal{BE}_{J/\psi}$	0.260	0.260	0%	
$m_b = 4.64$				
$m_\Upsilon$	9.46	9.46	0%	0%
$\mathcal{BE}_\Upsilon$	0.100	0.100	0%	

that would occur if the vertex dressing were to be generated by an explicit Feynman diagram structure. One would expect such a phenomenological LR kernel to be progressively too attractive when applied to meson with progressively heavier quarks.

The present model provides an opportunity to explore how much of the final meson mass result is attributable to vertex dressing and how this varies with quark mass. In Table II we display results for the ground state vector mesons in the u/d-, s-, c-, and b-quark regions for both rainbow-ladder truncation and the full model. Again the quark current masses are determined so that the full model reproduces experiment. We see that the amount by which the LR masses are too large decreases steadily with increasing quark mass, as expected. The LR truncation here is missing 6% of attraction for  $m_\phi$  compared to 21% in the restricted class of dressing diagram considered previously [14]. The LR truncation is quite accurate for the  $c\bar{c}$  and  $b\bar{b}$  vector states, as expected.

For the larger quark masses, the meson mass is dominated by the sum of the quark masses. We also express the results in a form that has this large mass scale removed. For each state in Table II, we display an effective binding energy defined as  $\mathcal{BE} = 2M_q(0) - m_V$ , where  $M_q(0)$  is the quark mass function obtained from the DSE solution at  $p^2 = 0$ , and  $m_V$  is the meson mass. Thus  $M_q(0)$  is being used as a rough measure of the constituent quark mass. The use of a single  $p^2$  point may well be an overestimate of constituent masses. Furthermore, our fitted current quark masses are on the upper edge of what is usually quoted at a renormalization scale of  $\mu = 2$  GeV [29]. Such an overestimate would be am-

TABLE III: The masses of the equal quark mass vector and pseudoscalar mesons in the u/d-, s-, c-, and b-quark regions, and the current quark masses required to reproduce the experimental vector meson masses. All are in units of GeV. The values of  $m_{\eta_c}$  and  $m_{\eta_b}$  are predictions. Experimentally [29],  $m_{\eta_c} = 2.9797 \pm 0.00015$  and  $m_{\eta_b} = 9.30 \pm 0.03$ . The fictitious pseudoscalar  $0_{ss}^-$  is included for comparison with other studies [14].

$m_{u,d} = 0.011$	$m_s = 0.165$	$m_c = 1.35$	$m_b = 4.64$
$m_\rho = 0.776$	$m_\phi = 1.02$	$m_{J/\psi} = 3.09$	$m_{\Upsilon(1S)} = 9.46$
$\mathcal{BE}_\rho = 0.311$	$\mathcal{BE}_\phi = 0.320$	$\mathcal{BE}_{J/\psi} = 0.260$	$\mathcal{BE}_\Upsilon = 0.100$
$m_\pi = 0.135$	$m_{0_{ss}^-} = 0.61$	$m_{\eta_c} = 2.97$	$m_{\eta_b} = 9.43$
$\mathcal{BE}_\pi = 0.953$	$\mathcal{BE}_{0^-} = 0.727$	$\mathcal{BE}_{\eta_c} = 0.380$	$\mathcal{BE}_{\eta_b} = 0.130$

plified in the infrared region via a DSE solution for the quark propagator. Nevertheless, a relative comparison should be meaningful. Table II shows the dependence of  $\mathcal{BE}$  upon the current quark mass for the fully dressed model and the ladder-rainbow truncation. On this basis, the relative amount of overbinding of the LR truncation is consistent with its relative lack of attraction with respect to the mass results.

In Table III we display the full model results for both the vector and pseudoscalar  $q\bar{q}$  states. The masses for  $\eta_c$  and  $\eta_b$  are predictions. In the c- and b-quark regions, these results are essentially the same as those of Ref. [14], because the differences in the employed model of vertex dressing become irrelevant when any dressing contribution is suppressed by the large mass of propagators internal to the vertex. The systematics of the mass dependence of hyperfine splitting that spans the c- and b-quark regions, here and in earlier work [14], strongly suggests that the experimental value [29],  $m_{\eta_b} = 9.30 \pm 0.03$ , is too low.

## V. SUMMARY

We have taken advantage of an algebraic model to enlarge the class of diagrams for the quark-gluon dressed vertex that can be incorporated into the Bethe-Salpeter kernel, while allowing a practical application to the calculation of meson masses. A given expansion of the vertex in diagrammatic form, produces a diagrammatic expansion of the quark self-energy, which in turn specifies a diagrammatic expansion of the BSE kernel if chiral symmetry is to be respected. This procedure relieves the phenomenology of the task of reproducing Goldstone's theorem whenever parameters are changed - it is always obeyed in this approach and thus phenomenology can address itself to a more constrained task. The constraints are considerable: a realistic ladder-rainbow kernel fitted to  $\langle\bar{q}q\rangle^0$  [3] produces  $m_\rho$ ,  $m_\phi$  and  $m_{K^*}$  to better than 5%. Such a phenomenological LR kernel for light mesons has absorbed vertex dressing but without the explicit  $m_q$  de-

pendence associated with an explicit diagrammatic representation of the dressed gluon-quark vertex. In order to gain more information it is necessary to work with a model that can implement a summation of vertex diagrams, turn that into a summation of diagrams for the chiral symmetry preserving BSE kernel, and allow a practical solution of the meson BSE.

To this end we use the Munczek-Nemirovsky Ansatz [15] for the interaction kernel. We use an improved model for the quark-gluon dressed vertex wherein each diagram for the dressed vertex has each of its internal vertices dressed in a self-consistent way. This moves considerably beyond the ladder BSE structure [14] for the vertex, in which vertices internal to the dressed vertex of interest are bare. In common with Ref. [14], we also use an effective method, with one parameter ( $\mathcal{C} = 0.15$  for this model), to accommodate the important non-Abelian effect of the 3-gluon coupling for the vertex. Quenched lattice-QCD data for the quark propagator and the quark-gluon vertex at zero gluon momentum fixed the parameter  $\mathcal{C}$ , while  $m_\pi$  and  $m_\rho$  fixed the other two parameters via the fully dressed vertex results.

The resulting model provides a laboratory within which the relevance of ladder-rainbow truncation (bare vertex) can be explored over a range of quark masses from u/d-quarks to b-quarks. The influence of the enlarged class of vertex dressing diagrams included in this work is seen to indicate that LR truncation is missing 9.5% of attraction for  $m_\rho$ , whereas the previous information from a smaller class of vertex dressing diagrams had LR missing 30% of attraction. The extra dressing diagrams included here tend to provide some cancellation, making the LR truncation somewhat more accurate. As heavier  $q\bar{q}$  mesons are considered, the amount of missing attraction in the LR truncation decreases steadily, as does the influence of vertex dressing—it is less than 1% for the  $J/\psi$  and  $\Upsilon$ .

The influence of the non-Abelian 3-gluon coupling is very significant. No attempt has been made to consider 4-gluon coupling nor to consider non-planar gluon line diagrams (e.g. crossed-box diagrams) for the vertex dressing. On the other hand, a limited class of non-planar gluon line diagrams for the meson BSE kernel, as generated from the planar diagrams of the dressed vertex, are included. While the complex task of including both planar and non-planar two-point gluon line diagrams for the vertex is currently underway, it is not yet known whether explicit 3- and 4-gluon couplings can be accommodated, even through the device of an effective color factor.

## Acknowledgments

This work was supported in part by DOE grant DE-AC05-84ER40150, under which SURA operates Jefferson Lab, the U.S. National Science Foundation under Grant Nos. PHY-0500291 and PHY-0301190 and the South-eastern Universities Research Association(SURA). HHM

thanks Jerry P. Draayer for his support during the course of the work, the Graduate School of Louisiana State University for a fellowship partially supporting his research, George S. Pogosyan and Sergue I. Vinitsky for their support at the Joint Institute of Nuclear Research. PCT

thanks the Theory Group of Jefferson Lab for support and hospitality during a sabbatical leave spent partly there in Fall 2005 and also thanks Craig Roberts for helpful conversations.

---

[1] P. Maris and C. D. Roberts, *Int. J. Mod. Phys. E* **12**, 297 (2003), nucl-th/0301049.

[2] J. Volmer et al. (The Jefferson Lab F(pi) Collaboration), *Phys. Rev. Lett.* **86**, 1713 (2001), nucl-ex/0010009.

[3] P. Maris and P. C. Tandy, *Phys. Rev. C* **62**, 055204 (2000), nucl-th/0005015.

[4] R. Alkofer, A. Holl, M. Kloker, A. Krassnigg, and C. D. Roberts, *Few Body Syst.* **37**, 1 (2005), nucl-th/0412046.

[5] D. Jarecke, P. Maris, and P. C. Tandy, *Phys. Rev. C* **67**, 035202 (2003), nucl-th/0208019.

[6] P. Maris and C. D. Roberts, *Phys. Rev. C* **56**, 3369 (1997), nucl-th/9708029.

[7] P. Maris, C. D. Roberts, and P. C. Tandy, *Phys. Lett. B* **420**, 267 (1998), nucl-th/9707003.

[8] C. D. Roberts and S. M. Schmidt, *Prog. Part. Nucl. Phys.* **45S1**, 1 (2000), nucl-th/0005064.

[9] R. Alkofer and L. von Smekal, *Phys. Rept.* **353**, 281 (2001), hep-ph/0007355.

[10] H. J. Munczek, *Phys. Rev. D* **52**, 4736 (1995), hep-th/9411239.

[11] A. Bender, C. D. Roberts, and L. Von Smekal, *Phys. Lett. B* **380**, 7 (1996), nucl-th/9602012.

[12] A. Bender, W. Detmold, C. D. Roberts, and A. W. Thomas, *Phys. Rev. C* **65**, 065203 (2002), nucl-th/0202082.

[13] P. Watson, W. Cassing, and P. C. Tandy, *Few Body Syst.* **35**, 129 (2004), hep-ph/0406340.

[14] M. S. Bhagwat, A. Holl, A. Krassnigg, C. D. Roberts, and P. C. Tandy, *Phys. Rev. C* **70**, 035205 (2004), nucl-th/0403012.

[15] H. J. Munczek and A. M. Nemirovsky, *Phys. Rev. D* **28**, 181 (1983).

[16] C. S. Fischer and R. Alkofer, *Phys. Rev. D* **67**, 094020 (2003), hep-ph/0301094.

[17] J. S. Ball and T.-W. Chiu, *Phys. Rev. D* **22**, 2542 (1980).

[18] D. C. Curtis and M. R. Pennington, *Phys. Rev. D* **42**, 4165 (1990).

[19] W. J. Marciano and H. Pagels, *Phys. Rept.* **36**, 137 (1978).

[20] J. I. Skullerud, P. O. Bowman, A. Kizilersü, D. B. Leinweber, and A. G. Williams, *JHEP* **04**, 047 (2003), hep-ph/0303176.

[21] J.-I. Skullerud, P. O. Bowman, A. Kizilersu, D. B. Leinweber, and A. G. Williams, *Nucl. Phys. Proc. Suppl.* **141**, 244 (2005), hep-lat/0408032.

[22] M. S. Bhagwat and P. C. Tandy, *Phys. Rev. D* **70**, 094039 (2004), hep-ph/0407163.

[23] A. I. Davydychev, P. Osland, and L. Saks, *Phys. Rev. D* **63**, 014022 (2001), hep-ph/0008171.

[24] J. M. Cornwall, R. Jackiw, and E. Tomboulis, *Phys. Rev. D* **10**, 2428 (1974).

[25] Wolfram, *Mathematica* 5.2 (2005), URL <http://www.wolfram.com>.

[26] R. Mertig, M. Bohm, and A. Denner, *Comput. Phys. Commun.* **64**, 345 (1991), URL <http://www.feyncalc.org>.

[27] P. O. Bowman, U. M. Heller, D. B. Leinweber, and A. G. Williams, *Nucl. Phys. Proc. Suppl.* **119**, 323 (2003), hep-lat/0209129.

[28] P. Maris and P. C. Tandy, *Phys. Rev. C* **60**, 055214 (1999), nucl-th/9905056.

[29] S. Eidelman et al. (Particle Data Group), *Phys. Lett. B* **592**, 1 (2004).